Role of small amount of MgO and ZrO$_2$ on creep behaviour of high purity Al$_2$O$_3$

L N SATAPATHY* and S SWAROOP[†]

Ceramic Technological Institute, Bharat Heavy Electricals Ltd., IISc Post, Bangalore 560 012, India
[†]Department of Metallurgy, Indian Institute of Science, Bangalore 560 012, India

Abstract. Small levels of various dopants have a significant effect on creep in polycrystalline alumina. While most previous studies have examined the effect of ionic size, the influence of valency of dopants on creep has not yet been completely characterized. The present detailed experimental study, utilizing magnesia and zirconia with a similar ionic size, demonstrates that the ionic valency of dopants also plays a crucial role in creep since magnesia does not significantly alter creep whereas zirconia retards creep substantially. Magnesia doped alumina deforms by Coble diffusion creep whereas zirconia doped alumina deforms by an interface controlled diffusion creep process.

Keywords. Alumina; zirconia; magnesia; creep; dopant.

1. Introduction

Ceramics are being considered increasingly for structural applications at elevated temperatures. Under such operating conditions, the time dependent plastic deformation of materials, termed creep, is an important design constraint. High temperature creep deformation is usually characterized in terms of the following expression

$$\dot{e} = \frac{ADGb}{kT}\left(\frac{b}{d}\right)^{p}\left(\frac{s}{G}\right)^{n},\qquad(1)$$

where $\dot{e}$ is the steady state strain rate, A a dimensionless constant, D the appropriate diffusion coefficient, G the shear modulus, b the magnitude of the Burgers vector, k the Boltzmann's constant, T the absolute temperature, d the grain size, s the imposed stress, and p and n are constants termed the inverse grain size exponent and stress exponent, respectively. The diffusion coefficient can be expressed as

$$D = D_0 \exp(-Q/RT),\qquad(2)$$

where D_0 is the frequency factor, Q the appropriate activation energy and R the gas constant.

Experimental studies on creep usually involve characterization of the parameters, n, p and Q, together with appropriate microstructural studies for identifying the rate controlling creep mechanisms. Typically, values of $n \geq 3$ are associated with intragranular dislocation creep and a value of $n = 1$ is associated with diffusion creep processes (Chokshi and Langdon 1991). In fine grained ceramics,

diffusion creep is likely to occur by matter transport along grain boundaries, as modelled by Coble (1963), and this process involves $n = 1$, $p = 3$ and $Q = Q_{gb}$, where Q_{gb} is the activation energy for grain boundary diffusion.

There have been numerous studies on creep in polycrystalline alumina (Cannon and Coble 1975; Kottada and Chokshi 2000), and creep has been attributed to either diffusion or interface controlled diffusion creep. Due to the high energies for formation of Frenkel and Schottky defects in alumina (Mackrodt 1984), it is anticipated that creep can be influenced significantly by doping alumina with small levels of other elements. Although some early studies suggested that the creep rate can be increased by doping alumina with Fe, Ti and Mn (Gordon 1984), more recent studies have demonstrated that the rates can be drastically reduced by some dopants such as Zr, Y and elements in the lanthanide series (Wakai *et al* 1988, 1997; French *et al* 1994; Cho *et al* 1997, 1999; Yoshida *et al* 1997, 1999, 2002a). It has been suggested that oversize dopants segregate to grain boundaries and retard creep by either modifying the strength of the ionic bonds or by reducing the grain boundary diffusion coefficient (Cho *et al* 1999; Yoshida *et al* 2002a,b).

Although most studies on creep in alumina with dopants have examined the effect of ionic size on creep, especially with isovalent additives, it is anticipated that both the ionic size (contributing to strain energy) as well as the valency (contributing to charge compensation) will influence defect formation, grain boundary segregation and diffusion in ionic solids.

Most of the recent studies have demonstrated that there is a significant increase in the activation energy with the addition of dopants, but there is not much information

---

*Author for correspondence (satpathy@bhelepd.com)

available on the stress exponents and grain size dependencies under similar conditions. Since the grain sizes of the undoped and doped aluminas are frequently not identical, a comparison of the relative creep rates with the same grain size is usually made by using an arbitrary value of the inverse grain size exponent, $p \sim 1$ to 3 (Wakai *et al* 1997; Cho *et al* 1997). A complete characterization of creep requires the evaluation of all three creep parameters (n, p and Q) so that the creep behaviour can be considered under similar values of grain size, stress and temperatures.

The present experimental investigation was undertaken specifically to examine the role of valency on creep in alumina, by conducting a complete study of creep in alumina doped with magnesia and zirconia.

2. Experimental

Magnesia and zirconia were chosen as the dopants to be examined in this study. Both have a ionic size of 0·072 nm compared with 0·054 nm for Al^{3+}, but different valencies (Mg^{2+} and Zr^{4+}). High purity *a*-alumina powder (99·99%) was obtained from Taimei Chemicals, Japan, with an average particle size of 0·2 *m*m. The impurities in the powder were Na-3, K-1, Fe-6, Ca-1, Mg-1 and Si-9 ppm.

Pure alumina (designated A) disks were prepared by cold compacting the powder at 40 MPa, and then by cold isostatic pressing at 120 MPa. The resultant green compact was sintered in air at 1773 K for 2 h. Some of the cold isostatically pressed alumina disks were sintered at 1673 K for 1 h and then at 1723 K for 1 h.

Magnesia doped alumina (designated AM250) was prepared by dissolving a pre-determined amount of magnesium nitrate and alumina powder in de-ionized water, to eventually obtain alumina doped with 250 ppm of magnesia. The resultant solution was kept at 373 K for 10 h to eliminate water and later calcined at 973 K for 2 h. The magnesia doped alumina powder thus obtained was mixed with polyethylene glycol (PEG) binder and cold compacted at 80 MPa. The compact was further cold isostatically pressed at 120 MPa and then sintered in air at 1773 K for 1 h.

Alumina doped with 1000 ppm zirconia (designated AZ1000) was prepared by ball milling for 24 h, using zirconia balls, a mixture of 3 mol% yttria stabilized tetragonal zirconia, alumina and isopropyl alcohol. The dried powder was sieved, mixed with PEG, cold compacted at 30 MPa, and cold isostatically pressed at 110 MPa. The compacts were sintered at 1773 K for 2 h.

Care was taken during all processing steps to avoid contamination by using plastic ware. The densities of the samples were measured by Archimedes method. For microscopy, polished samples were thermally etched at 1823 K/1 h for pure alumina and 1673 K/2 h for magnesia doped alumina. Some pure alumina samples and all zirconia doped alumina samples were thermally etched at 1773 K for 1 h. Evaluation of the grain growth kinetics suggested that the thermal etching process did not lead to grain growth. Optical and scanning electron microscopies were used for characterizing the microstructure. Mean linear intercept grain sizes were measured along the horizontal ($\bar{L}_h$) and vertical ($\bar{L}_v$) directions, and the average grain size was defined as $\bar{L} = (\bar{L}_h^2 \bar{L}_v)^{1/3}$. For the deformed samples ($\bar{L}_v$) corresponded to the compression axis.

Samples for creep testing were cut from the sintered disk, with a nominal height to diameter ratio of 1·5. The method of constant stress compression creep testing is detailed elsewhere (Owen and Chokshi 1991). The range of experimental parameters studied were: stress from 10 to 200 MPa, grain size from ~ 1·5 to 10 *m*m and temperature from 1623 to 1773 K.

3. Results and discussion

The as-sintered A disks were > 98% dense, whereas the AM250 and AZ1000 disks were > 99% dense. X-ray diffraction and scanning electron microscopy of all the three materials revealed the presence of only the *a*-alumina phase. The grain sizes of the as-sintered materials were ~ 2, 1·5 and 2·5 *m*m for A, AM250 and AZ1000, respectively, and the grains were equiaxed in the three materials.

Table 1 provides details on the experimental conditions together with mechanical and microstructural data for the
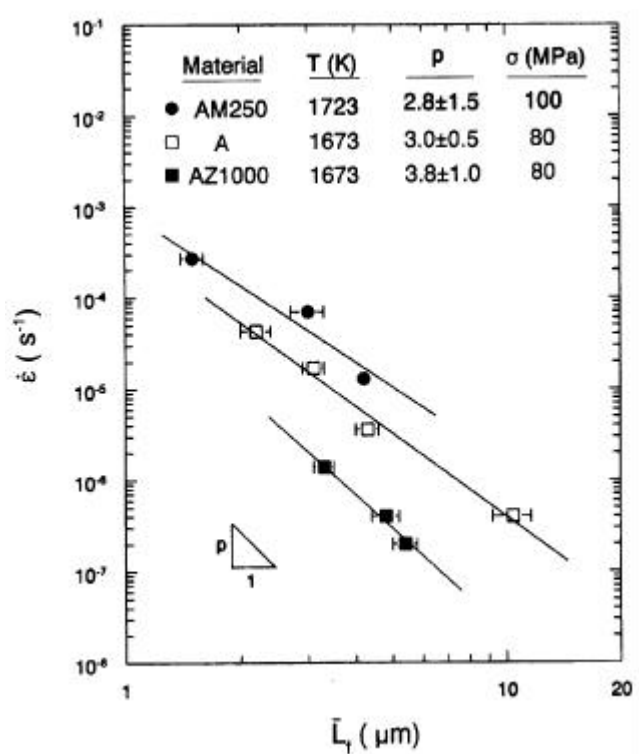
Table 1. High temperature deformation behaviour of Al_2O_3 + 1000 ppm ZrO_2.

T (K)	s (MPa)	e (%)	t (s)	$\dot{e}$ (s^{-1})	r_0 (g/cc)	r_f (g/cc)	$\bar{L}_0$ (µm)	$\bar{L}_f$ (µm)	Aspect ratio
1673	10	3·0	328590	$8·0 \times 10^{-8}$	3·98	3·89	2·5 ± 0·2	3·0 ± 0·2	1·06
1673	20	8·3	422590	$2·0 \times 10^{-7}$	3·98	3·95	2·5 ± 0·2	3·3 ± 0·2	1·04
1673	40	7·5	106770	$6·5 \times 10^{-7}$	3·98	NA	2·5 ± 0·2	NA	NA
1673	80	7·9	46810	$1·4 \times 10^{-6}$	3·98	3·92	2·5 ± 0·2	3·2 ± 0·2	1·07
1673	200*	7·0	6900	$1·4 \times 10^{-5}$	3·98	3·80	2·5 ± 0·2	3·5 ± 0·2	1·10
1673	80	10·0	164580	$1·2 \times 10^{-6}$	NA	NA	NA	4·8 ± 0·2	1·10
1673	80	1·2	64430	$1·8 \times 10^{-7}$	NA	3·88	NA	5·4 ± 0·2	1·14
1623	80	14·5	159580	$6·4 \times 10^{-7}$	3·98	NA	2·5 ± 0·2	2·9 ± 0·3	1·10
1723	80	15·1	27990	$5·5 \times 10^{-6}$	3·98	3·86	2·5 ± 0·2	3·8 ± 0·4	1·11

*Sample fractured during testing; r_0 and r_f are the initial and final densities, respectively; NA: not available.

AZ1000 samples. The initial and final grain sizes are listed as $\overline{L}_0$ and $\overline{L}_f$, respectively, and the aspect ratio was defined as $\overline{L}_h / \overline{L}_v$. Similar details were also obtained for the pure alumina and magnesia doped alumina samples. Inspection of the data shown in table 1 indicates that there was not much grain growth, except in the sample tested at 1723 K. There was very little grain growth in the magnesia doped alumina and the coarser grained pure alumina. Consequently, tests on the zirconia doped alumina were performed largely at 1673 K whereas experiments on the magnesia doped alumina were conducted largely at 1723 K. Microstructural observation indicated also that the grains retained their equiaxed shapes after substantial compressive strains. There was not much change in the density of the samples, except for the test conducted at a high stress of 200 MPa. Similar observations were also made in the pure alumina and magnesia doped alumina.

There was a very short primary region to strains of ~ 1%, and there was good evidence for steady state deformation under most experimental conditions. Figure 1 illustrates the variation in final strain rate with final grain size on a logarithmic scale for all three materials. It is clear that there was considerable scatter in the data for the doped materials. Since there are no theoretical models involving a value of $p \sim 4$, it is reasonable to consider deformation with $p \sim 3$ also for the zirconia doped alumina. Consequently, within experimental scatter, the inverse grain size exponent is $p \sim 3$ for all materials.
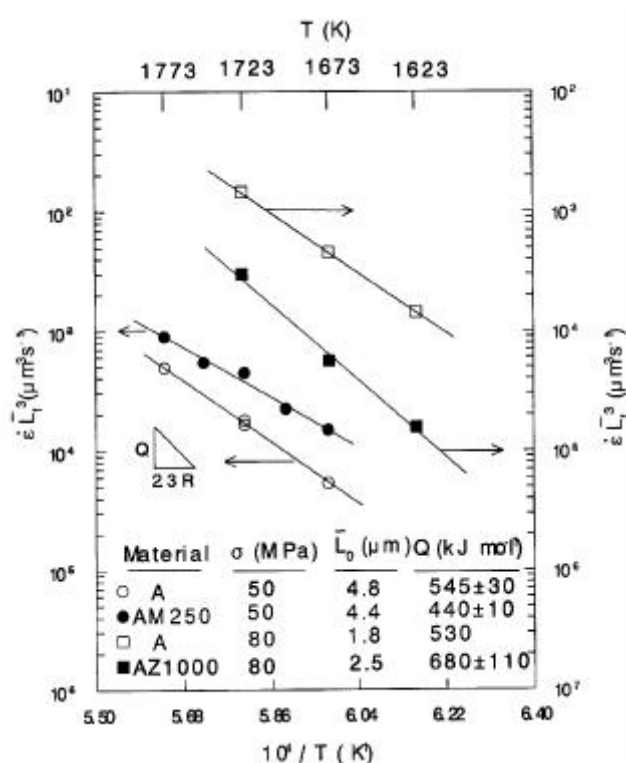
In order to account for the changes in grain size during creep, it follows from (1) that the activation energy may be obtained from an Arrhenius plot of the variation in the parameter $\dot{e}\,\overline{L}_f^{\,p}$ with inverse temperature. Such a plot is shown in figure 2 for all three materials with $p = 3$. It is clear that while the activation energy of the pure alumina and magnesia doped alumina is ~ 500 kJ mol⁻¹, the value is much higher (680 kJ mol⁻¹) for the zirconia doped alumina.

Figure 3 illustrates on a logarithmic scale the variation in the parameter, $\dot{e}\,\overline{L}_f^{\,3}$, with stress at temperatures of 1673 and 1723 K. In addition, the theoretical Coble diffusion creep rates are shown as dashed lines, and these are discussed later. There are two important points to note from this figure. First, while magnesia doping enhances the creep rate of alumina by a factor of less than ~ 3, zirconia doping reduces the creep rate by a factor of up to ~ 20. Second, while pure alumina and magnesia doped alumina are associated with a stress exponent of ~ 1, creep in the zirconia doped alumina involves a value of $n \sim 2$.

There was no evidence of the formation of second phases in either the magnesia doped or zirconia doped aluminas. Although the solubility of magnesia and zirconia in alumina is very limited (Levin *et al* 1969), the present experimental observations of lack of second phases is consistent with previous studies which have shown also that Mg and Zr segregate to grain boundaries in such materials (Takigawa *et al* 1997; Wakai *et al* 1997; Yoshida *et al* 2002a).

Figure 1. Variation in the final strain rate with final grain size for pure alumina, magnesia doped alumina and zirconia doped alumina.

Figure 2. Variation in the grain size compensated strain rate with inverse temperature for the three materials.

The experimental observations of $n \sim 1$ and $p \sim 3$ are consistent with Coble grain boundary diffusion creep, which predicts the following creep rate, $\dot{e}_{\mathrm{co}}$ (Coble 1963)

$$\dot{e}_{\mathrm{co}} = \frac{33 \boldsymbol{d} D_{\mathrm{gb}}}{kT} \left(\frac{b}{d} \right)^3 \boldsymbol{s} , \qquad (2)$$

where $\boldsymbol{d}$ is the grain boundary width. The theoretical Coble creep rates are also shown in figure 3 as dashed lines, using the grain boundary diffusion coefficient reported by Cannon and Coble (1975) and defining the spatial grain size, $d = 1 \cdot 74 \, \overline{L}$. It is quite clear from figure 3 that the experimental creep rates for pure alumina are in agreement with the theoretical predictions to within a factor of ~ 2. Although conventional topological models for diffusion creep suggest that grains should elongate along the tensile axis, there are other topological considerations that can lead to a retention of the equiaxed grain size during diffusion creep (Chokshi 2000).

Inspection of figure 3 reveals also that the magnesia doped alumina deforms at a creep rate of up to three times that for pure alumina. It has also been demonstrated recently that creep in magnesia doped alumina is consistent with the Coble creep model (Kottada and Chokshi 2000), although the absolute creep rates were up to a factor of ~ 4 higher than the predictions based on the grain boundary diffusion coefficient reported by Cannon and Coble (1975). Experiments on alumina have shown that there is a scatter of up to a factor of ~ 2 in creep rates for tests conducted under nominally similar conditions. Consequently, it is

Figure 3. Variation in the grain size compensated strain rate with stress for the three materials. Also shown are theoretical calculations based on Coble diffusion creep (dashed lines).

concluded that magnesia does not have any significant influence on creep in alumina. In addition, it is to be noted that the segregation of magnesia to grain boundaries does not significantly alter the activation energy for grain boundary diffusion.

Doping alumina with zirconia leads to a significant decrease in creep rate, an increase in the activation energy and an increase in the stress exponent. The significant decrease in creep rate and the increase in activation energy are consistent with many previous reports on zirconia doped alumina (Wakai *et al* 1988, 1997; Yoshida *et al* 1997). However, this is the first report of a change in rate controlling process in zirconia doped alumina. In pure alumina, it has been shown that deformation occurs by the sequential combination of diffusion creep and interface controlled diffusion creep, such that there is a transition from $n \sim 2$ to $n \sim 1$ with an increase in stress (Cannon *et al* 1980). The present observations of a decrease in creep rate and an increase in stress exponent are consistent with an interface controlled diffusion creep process. Owing to rapid fracture at high stresses, it was not possible in the present study to experimentally examine the possibility of a decrease in stress exponent to $n \sim 1$ at higher stresses. In this context, it is interesting to note that a very recent study on alumina bicrystals has demonstrated that Y segregation to grain boundaries reduced the grain boundary sliding rate by two orders of magnitude (Matsunaga *et al* 2003).

Based on the present experimental investigation, it is clear that magnesia and zirconia have a substantially different effect on creep although they have a similar ionic size. Therefore, in addition to ionic size (contributing to strain energy), it is necessary to also consider the ionic valency (contributing to charge compensation) of the segregating dopant. Theoretical models for the influence of ionic size and valency using model clusters have suggested that the increase in ionic bond strength is responsible for a decrease in creep rate (Yoshida *et al* 2002a,b; Fabris and Elsasser 2003). However, to date such models have not taken into account the combined effect of the structure of grain boundaries, the charge compensating defects produced thereby introducing aliovalent dopants, the local coordination of the segregating ions, and the possibility of defect clusters. This is clearly an important area for further investigation.

Finally, it is interesting to note that although both magnesia and zirconia doping retard grain growth in alumina, they have a substantially different effect on creep deformation. A similar difference in creep and grain growth has also been noted recently in yttria stabilized tetragonal and cubic zirconia (Chokshi 2003).
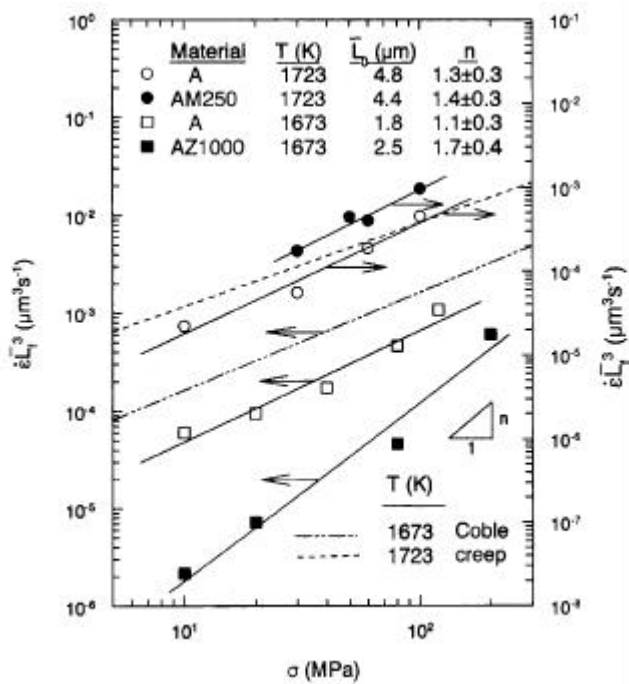
4. Conclusions

Detailed experiments were conducted to characterize the creep behaviour of pure alumina and alumina doped with magnesia or zirconia. Creep of pure alumina is consistent

with Coble grain boundary diffusion creep. Although both magnesia and zirconia have a similar ionic size, and both are oversized with respect to Al, magnesia doping slightly increases the creep rate whereas zirconia doping substantially reduces the creep rate in alumina. It is clear that, together with the ionic size, the ionic valency also needs to be considered in evaluating the influence of dopants on creep in alumina.

Acknowledgements

References

Cannon R M and Coble R L 1975 *Deformation of ceramic materials* (eds) R C Bradt and R E Tressler (New York: Plenum Press) pp 61–100

Cannon R M, Rhodes W H and Heuer A H 1980 *J. Am. Ceram. Soc.* **63** 46

Cho J, Harmer M P, Chan H M, Rickman J M and Thompson A M 1997 *J. Am. Ceram. Soc.* **80** 1013

Cho J, Wang C M, Chan H M, Rickman J M and Harmer M P 1999 *Acta Mater.* **47** 4197

Chokshi A H 2000 *Scr. Mater.* **42** 241

Chokshi A H 2003 *Scr. Mater.* **48** 791

Chokshi A H and Langdon T G 1991 *Mater. Sci. Technol.* **7** 577

Coble R L 1963 *J. Appl. Phys.* **34** 1679

Fabris S and Elsasser C 2003 *Acta Mater.* **51** 71

French J D, Zhao J, Harmer M P, Chan H M and Miller G A 1994 *J. Am. Ceram. Soc.* **77** 2857

Gordon R S 1984 *Advances in ceramics* (Columbus, Ohio: American Ceramic Society) **10**, p. 418

Kottada R S and Chokshi A H 2000 *Acta Metall. Mater.* **48** 3905

Levin E M, Robins C R and Mc Murdie H F 1969 *Phase diagram for ceramics* (Columbus, Ohio: American Ceramic Society)

Mackrodt W C 1984 *Advances in ceramics* (Columbus, Ohio: American Ceramic Society) **10**, p. 62

Matsunaga K, Nishimura H, Muto H, Yamamoto T and Ikuhara Y 2003 *Appl. Phys. Lett.* **82** 1179

Owen D M and Chokshi A H 1991 *Superplasticity in advanced materials* (eds) S Hori, M Tokizane and N Furushiro (Osaka: The Japan Society for Research on Superplasticity) p. 171

Takigawa Y, Ikuhara Y and Sakuma T 1997 *Mater. Sci. Forum* **243–245** 425

Wakai F, Nagano T and Iga T 1988 *J. Ceram. Soc. Japan* **96** 1206

Wakai F, Nagano T and Iga T 1997 *J. Am. Ceram. Soc.* **80** 2361

Yoshida H, Okada K, Ikuhara Y and Sakuma T 1997 *Philos. Mag. Lett.* **76** 9

Yoshida H, Ikuhara Y and Sakuma T 1999 *Philos. Mag. Lett.* **79** 249

Yoshida H, Ikuhara Y and Sakuma T 2002a *Acta Metall. Mater.* **50** 2955

Yoshida H, Yamamoto T, Ikuhara Y and Sakuma T 2002b *Philos. Mag. Lett.* **82** 511